Journal of Hazardous Materials 263 (2013) 702–710

Contents lists available at ScienceDirect

Journal of Hazardous Materials

journal homepage: www.elsevier.com/locate/jhazmat

Adsorption of selected endocrine disrupting compounds and pharmaceuticals on activated biochars

Chanil Jung[a], Junyeong Park[b], Kwang Hun Lim[c], Sunkyu Park[b], Jiyong Heo[d], Namguk Her[e], Jeill Oh[f], Soyoung Yun[f], Yeomin Yoon[a,*]

[a] Department of Civil and Environmental Engineering, University of South Carolina, Columbia, SC 29208, USA
[b] Department of Forest Biomaterials, North Carolina State University, Raleigh, NC 27695, USA
[c] Department of Chemistry, East Carolina University, Greenville, NC 27858, USA
[d] Department of Civil and Environmental Engineering, Korea Army Academy at Young-Cheon, PO Box 135-1, Changhari, Gogyeongmeon, Young-cheon 770-849, Gyeongbuk, South Korea
[e] Department of Chemistry and Environmental Sciences, Korea Army Academy at Young-Cheon, PO Box 135-1, Changhari, Gogyeongmeon, Young-cheon 770-849, Gyeongbuk, South Korea
[f] Department of Civil and Environmental Engineering, Chung-Ang University, Dongjak-Ku, Seoul 156-756, South Korea

HIGHLIGHTS

- Biochars were prepared at different gas environments.
- The competitive adsorption among EDCs/PhACs were investigated.
- Aromaticity of adsorbent plays a significant role for EDCs/PhACs adsorption.

GRAPHICAL ABSTRACT

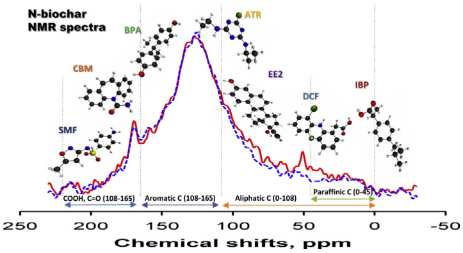

ARTICLE INFO

Article history:
Received 23 July 2013
Received in revised form 14 October 2013
Accepted 17 October 2013
Available online 24 October 2013

Keywords:
Endocrine disrupting compounds
Pharmaceuticals
Biochar
Nuclear magnetic resonance
Adsorption mechanism

ABSTRACT

Chemically activated biochar produced under oxygenated (O-biochar) and oxygen-free (N-biochar) conditions were characterized and the adsorption of endocrine disrupting compounds (EDCs): bisphenol A (BPA), atrazine (ATR), 17 α-ethinylestradiol (EE2), and pharmaceutical active compounds (PhACs); sulfamethoxazole (SMX), carbamazepine (CBM), diclofenac (DCF), ibuprofen (IBP) on both biochars and commercialized powdered activated carbon (PAC) were investigated. Characteristic analysis of adsorbents by solid-state nuclear magnetic resonance (NMR) was conducted to determine better understanding about the EDCs/PhACs adsorption. N-biochar consisted of higher polarity moieties with more alkyl (0–45 ppm), methoxyl (45–63 ppm), O-alkyl (63–108 ppm), and carboxyl carbon (165–187 ppm) content than other adsorbents, while aromaticity of O-biochar was higher than that of N-biochar. O-biochar was composed mostly of aromatic moieties, with low H/C and O/C ratios compared to the highly polarized N-biochar that contained diverse polar functional groups. The higher surface area and pore volume of N-biochar resulted in higher adsorption capacity toward EDCs/PhACs along with atomic-level molecular structural property than O-biochar and PAC. N-biochar had a highest adsorption capacity of

---

Abbreviations: ATR, atrazine; BET, Brunauer–Emmett–Teller; BPA, Bisphenol A; CBM, carbamazepine; DCF, diclofenac; DP/MAS, direct polarization/magic angle spinning; EDCs, endocrine disrupting compounds; EE2, 17α-ethinylestradiol; HCl, hydrochloric acid; IBP, ibuprofen; NaOH, sodium hydroxide; NMR, nuclear magnetic resonance; NOMs, natural organic matters; PAC, powdered activated carbon; PhACs, pharmaceutically active compounds; SMX, sulfamethoxazole.

* Corresponding author. Tel.: +1 803 777 8952; fax: +1 803 777 0670.
E-mail address: yoony@cec.sc.edu (Y. Yoon).

0304-3894/$ – see front matter © 2013 Elsevier B.V. All rights reserved.
http://dx.doi.org/10.1016/j.jhazmat.2013.10.033

all chemicals, suggesting that N-biochar derived from loblolly pine chip is a promising sorbent for agricultural and environmental applications. The adsorption of pH-sensitive dissociable SMX, DCF, IBP, and BPA varied and the order of adsorption capacity was correlated with the hydrophobicity (K_{ow}) of adsorbates throughout the all adsorbents, whereas adsorption of non-ionizable CBM, ATR, and EE2 in varied pH allowed adsorbents to interact with hydrophobic property of adsorbates steadily throughout the study.

© 2013 Elsevier B.V. All rights reserved.

1. Introduction

Endocrine-disrupting compounds (EDCs) and pharmaceutically active compounds (PhACs) are trace-level organic contaminants that have been detected in aquatic environments such as surface waters, wastewater, runoff, and landfill leachates [1–3]. The widespread occurrence of these dissolved chemicals in water sources is of concern due to their adverse effects, such as mimicking or antagonizing natural hormones, hindering metabolic processes, occupying hormone receptors, and causing reproductive and development problems when consumed by humans and aquatic species [4,5].

A variety of EDCs exist, including pesticides, natural hormones, and industrial chemicals. Atrazine (ATR) is one of the most widely used herbicides and its continuous exposure into water causes its concentration to accumulate due to its poor degradability compared to other herbicides [6]. Recently, 17α-ethinylestradiol (EE2), an oral contraceptive, has been studied extensively due to its higher toxicity compared to other hormones such as estrone or 17β-estradiol [7]. Similarly, bisphenol A (BPA), a main monomer in epoxy resin and polycarbonate plastic, has been studied due to the ubiquitous use of plastic in everyday living. In addition, because of the increasing demand for PhACs, the level of exposure has increased, paradoxically causing a threat to health. Certain pharmaceuticals have been studied widely, such as non-steroidal anti-inflammatory drugs; diclofenac (DCF) and ibuprofen (IBP), as well as antibiotics (sulfamethoxazole; SMX) and anti-seizure medicine (carbamazepine; CBM). EDCs/PhACs are metabolized and adsorbed by organisms at low levels, resulting in exposure to the residues of these compounds as their origin molecular forms or their transformed products when they enter the aquatic environment [3,8]. Unfortunately, the treatment of EDCs/PhACs in wastewater and drinking water is inefficient [9,10] and consequently more effective technologies are required to achieve their removal from drinking water.

Adsorption with a high-binding adsorbent has been used to eliminate various contaminants in the aqueous phase [11]. The well-established manufacturing process and relatively low cost of activated carbon has led to it becoming a common adsorbent for water treatment due to its strong interaction with hydrophobic organic contaminants. However, the physical properties of activated carbon, including the irregular and closed pore structure with small micropore sizes (<2 nm), precludes the adsorption of large molecules, leading to a size-exclusion effect [12]. The improvement of this crucial role of pore size for the adsorption has been studied through physical and chemical activation of adsorbents [13,14].

With an advance of biorefinery in the near future, it is expected to have biochar available for precursors for value-added products. Biochar is the by-product of the pyrolytic processing of biomass to obtain biofuel such as controlled thermal process and gasification, and has a potential as a promising adsorbent for the elimination of micro-pollutants due to its superior properties including a highly condensed structure and surface density of functional groups, although its activated product provides a lower surface area and volume than commercialized activated carbon [15,16]. These properties are controlled by the pyrolysis conditions (residence time and temperature), activation, and type of feedstock; biochar pyrolyzed at a high temperature consists mainly of polyaromatic carbons and has a higher microporosity, which enhances the adsorption of organic compounds, while higher proportions of aliphatic carbons and functional groups are typical of biochars pyrolyzed at a low temperature [16,17]. A separate study has shown that chemically activated biochar resulted in higher porous structure, surface area, and lower ash content than commercialized activated carbon [18]. Since most of organic forms such as any kind of plants, domestic and industrial wastes, sewage sludge, and animal manures have used as a source in pyrolysis, their composition of elements and ratio of inorganic compounds in biomass varies the both product yield and quality of bio-oil and biochar [19]. The overall objective of this study was to characterize activated biochars produced in a laboratory, where biochars were prepared at different gas environments using conventional analytical methods as well as advanced solid-state nuclear magnetic resonance (NMR) techniques and how these properties determine the competitive adsorption characteristics and mechanisms of EDCs/PhACs. Commercialized powdered activated carbon (PAC) was also examined as a comparison. Seven EDCs/PhACs commonly occurring in the aquatic environment were selected as adsorbates and the effects of their hydrophobicity and molecular size on adsorption capacity were also investigated. The competitive adsorption among EDCs/PhACs were investigated in terms of characteristic difference both adsorbents and adsorbates. Furthermore, adsorption inhibition by natural organic matters (NOMs), described by humic acid, in this study was determined for better understanding in real wastewater condition.

2. Materials and methods

2.1. Target adsorbates

Three EDCs (BPA, ATR, and EE2) and four PhACs (SMX, CBM, DCF, and IBP) were purchased from Sigma–Aldrich (St. Louis, MO, USA). Although the seven compounds have similar molecular weights (206–296 g/mol), their pK_a values and octanol–water partition coefficients (K_{ow}) cover broad ranges. Detailed physicochemical properties are provided in Supporting Information (Table S1).

2.2. Adsorbents

The N- and O-biochar samples were produced through the thermal treatment of torrefied loblolly pine chips (15 mm × 6 mm) containing bark at 300 °C for 15 min in a laboratory-scale batch tube-furnace (OTF-1200X, MTI Corporation, Richmond, CA, USA), under pure nitrogen (N-biochar) and 7% oxygen + 93% nitrogen atmospheres (O-biochar). Due to the limitation of the loadable amount of samples in the tube furnace, N-/O-biochars were generated with several batches. After each batch, the weight loss from the thermal treatment was measured, and then the samples with a difference of ±3% in weight loss were collected for further experiments. The yields for N-/O-biochar were 42.3% and 64.2%, respectively. 3 g of each pyrolyzed biochar was activated with 40 mL of 4 M NaOH for 2 h and dried overnight at 105 °C. The NaOH-impregnated biochar samples were then heated at 800 °C for 2 h under a nitrogen gas flow (2 L/min) and cooled down (10 °C/min) after being separated from the solution using a Buchner filter funnel. The dried samples were rinsed with 0.1 M HCl followed by deionized water until they reached neutral pH, dried at 105 °C, milled and passed through a 74-μm sieve. Coal-based virgin, high-performance PAC, Calgon WPH® (Pittsburgh, PA, USA) was used to compare its adsorption ability with that of the biochars manufactured in the lab.

2.3. Characterization of adsorbents

Elemental analysis was performed using a PerkinElmer 2400 Series II Elemental Analyzer (PerkinElmer, Waltham, MA, USA). Oxygen content was calculated by subtracting the ash and carbon, hydrogen, and nitrogen contents from the total mass of the samples. The BET surface area was measured with a Gemini VII 2390p surface area analyzer (Micromeritics, Norcross, GA, USA) and the total pore volume was calculated from the adsorbed quantity of N_2 at $P/P_0 = 0.95$. Solid-state ^{13}C direct polarization/magic angle spinning (DP/MAS) NMR spectra were acquired with a 3.2 mm MAS probe, on a Varian Inova 500 spectrometer (Palo Alto, CA, USA). The ^{13}C NMR spectra combined with dipolar-recoupled NMR methods were used for quantitative structural analyses of the biochars and PAC. Detailed experimental conditions for the NMR experiments are described elsewhere [20].

2.4. Adsorption experiments

Adsorption isotherms of the EDCs and PhACs on the adsorbents were undertaken through batch experiments as described in our previous study [21] with a mixture of five different initial concentrations (10–50 μM). Each stock solution (10 mM), prepared in deionized water for DCF, and in acetonitrile for the others, was evaporated to minimize any cosolvent effect prior to addition to a 40-mL amber EPA vial equipped with a polytetrafluorethylene-lined screw cap. The pH and conductivity of aqueous background solution were adjusted using 1 N HCl or NaOH, and 0.1 M NaCl (to 150 μS/cm), respectively. A stock suspension of 2000 mg/L of each adsorbent (N/O-biochar and PAC) was prepared by adding 200 mg of each adsorbent to 100 mL of ultrapure deionized water (resistivity ~18 MΩ/cm) and mixing over a magnetic stirrer at 500 rpm, and added to each vial at 50 mg/L. After capping (leaving minimal headspace), the vials were mixed under ambient conditions for 7 days and allowed to reach apparent equilibrium. The effect of natural organic matter (NOM) was determined by spiking 5.0 mg/L humic acid (Sigma–Aldrich) as dissolved organic carbon with 10 μM EDCs/PhACs mixed solution.

Single batch experiments were conducted to determine the adsorption kinetics for EDCs/PhACs on N-biochar, O-biochar, and PAC. Solutions of EDCs/PhACs (10 μM each in 1000 mL) in beakers were transferred, and then the stock solution of each adsorbent was spiked to achieve 50 mg/L. The pH and conductivity were adjusted as described above. Under ambient conditions, the solutions were mixed over a magnetic stirrer at 150 rpm and sampled repeatedly at specific times. All adsorption experiments were conducted in duplicate.

After mixing, each aliquot was collected from the solution and filtered through a 0.22-μm Durapore® membrane filter (Millipore, Cork, Ireland), placed in a 2-mL amber vial, and analyzed using a high-performance liquid chromatograph equipped with a ultra-violet detector and a 4.6 mm × 150 mm LiChrosper RP-18 5 μm column (Agilent, Santa Clara, CA, USA) at a constant flow rate of 0.75 mL/min for 23 min. The mobile phase was 5 mM phosphoric acid:acetonitrile (50:50, v/v). The detector wavelength was set at 210 nm for all EDCs and PhACs; SMX, CBM, BPA, ATR, EE2, DCF, and IBP eluted from the column at 3.8, 5.4, 7.1, 9.4, 10.6, 19.0, and 21.0 min, respectively.

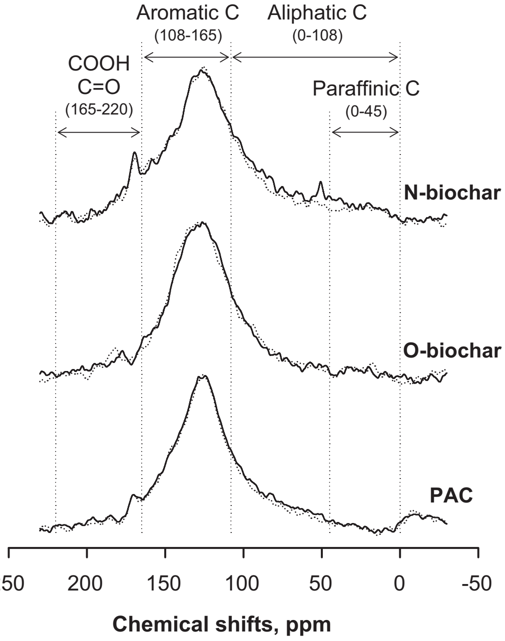

Fig. 1. Solid-state ^{13}C DP/MAS NMR spectra (solid line) with corresponding recoupled ^{1}H-^{13}C dipolar dephasing spectra (dotted line) for N-/O-biochars and PAC samples.

2.5. Data analysis

The adsorption isotherms were analyzed with the Freundlich isotherm model (Eq. (1)).

$$q_e = K_F C_e^{1/n} \tag{1}$$

where q_e (mg/g) and C_e (mg/L) are the concentration of adsorbate in adsorbent and solution at equilibrium condition, respectively. K_F (mg/g) and n provide a unit adsorption capacity parameter and dimensionless intensity of the adsorbent parameter, respectively. In general, high value of K_F is indicative of favorable adsorption processes, while the reciprocal of n has a meaning of the surface heterogeneity (homogeneous surface; $n = 1$).

Pseudo-second-order model was employed to analyze the kinetics of adsorption (Eq. (2)).

$$\frac{t}{q_t} = \frac{1}{k_2 q_e^2} + \frac{1}{q_e} \tag{2}$$

where q_t and q_e are the amount of EDCs/PhACs adsorbed (mg/g) at time t and equilibrium condition, respectively, while k_2 is the pseudo-second-order model rate constant (g/h mg) for the adsorption.

3. Results and discussion

3.1. Characterization of adsorbents

The activated biochars produced from two different precursor biochars were characterized by elemental analyses and solid-state NMR. The elemental composition and ^{13}C NMR spectra of N-/O-biochars and PAC were markedly different (Fig. 1). The precursor biochar for the activated O-biochar was pyrolyzed in the presence of oxygen (3%), allowing the material to be partly combusted rather than fully charred [16]. This nominal oxidation resulted in a significant difference in pyrolysis (Table 1). The oxygen content (13.0%)

Table 1
Elemental composition, aromatic ratio, ash content, aromaticity, BET-N_2 surface area (SA-N_2), and cumulative pore volume of the adsorbents used in this study.

Samples	C (%)	H (%)	N (%)	O (%)	H/C	Polarity index		Ash (%)	Aromaticity[a]	SA-N_2[b] (m^2/g)	Pore volume[c] (cm^3/g)	
						N/C	O/C				Micro-pore	Macro-pore
N-Biochar	72.6	0.77	0.65	21.3	0.127	0.001	0.221	4.7	62.5	1360.3	0.307	0.643
O-Biochar	83.8	0.24	0.30	13.0	0.034	0.003	0.116	2.7	74.1	1150.7	0.313	0.318
PAC	59.3	0.16	0.31	20.2	0.032	0.004	0.255	20.1	69.4	972.3	0.216	0.314

[a] Aromaticity = 100 × aromatic C (108–165 ppm)/[aromatic C (108–165 ppm) + aliphatic C (0–108 ppm)]. Data of aromatic C (108–165 ppm) and aliphatic C (0–108 ppm) are listed in Table S2.

[b] Calculated using the Brunauer–Emmett–Teller (BET) equation for data in the range less than 0.1 of relative pressure.

[c] Calculated from the adsorbed quantity of N_2 at $P/P_0 = 0.95$ with *t*-plot mod.

of the O-biochar was lower than the N-biochar (21.3%), resulting in carbon contents of 83.8% and 72.6%, respectively. The H/C ratio of 0.034 for O-biochar, and 0.127 for N-biochar indicated that O-biochar was slightly more carbonized than N-biochar.

The elemental analyses are consistent with ^{13}C solid-state NMR results (Tables S2 and S3). The ^{13}C DP/MAS NMR spectra showed that O-biochar has more aromatic characters on the basis of a stronger peak at 108–148 ppm corresponding to aryl carbons than others. On the other hand, N-biochar has relatively higher aliphatic carbon fractions; paraffinic or alkyl (0–45 ppm), methoxyl (45–63 ppm), carbohydrate (63–108 ppm) and carboxyl carbons (165–187 ppm). Quantitative analyses of the ^{13}C DP/MAS and dipolar dephasing experiments showed that O-biochar has a more condensed aromatic structure with higher aromaticity based on the larger non-protonated carbon fraction, which agrees well with its lower H/C and O/C ratios than those of N-biochar. These results indicate that O-biochar has a higher hydrophobicity than N-biochar.

Porous structures (BET surface area and pore volume) of the activated biochars and PAC were examined by N_2 adsorption experiments (Table 1). The chemically activated N-/O-biochars exhibit fairly large surface area (1360.3 and 1150.7 m^2/g) and pore volume (0.95 and 0.63 cm^3/g, respectively) that are comparable or better than those of commercial activated carbons (972.3 m^2/g and 0.53 cm^3/g). It is notable that N-biochar with relatively lower aromaticity has a higher surface area and pore volume, suggesting aromatic structures may not help develop porous structures of biochar. The high surface area and pore volume of the biochars render the activated carbons from the renewable biomass a promising sorbent that can potentially replace coal-based activated carbons such as PAC. In addition, the amount of ash in the activated biochar is far lower than the commercial PAC. The low ash content of both N-/O-biochar (4.2 and 2.7%, respectively) were derived from its property as a feedstock; following the order of soft wood < hard wood < corn or wheat stover < livestock manure [19]. 20.1% ash content of coal-based PAC hardly contributes to hydrophobic organic compounds, excepting for the interaction of ash-preferring species such as dyes and metal ions [22,23]; therefore, not only the effective surface area and pore volume of adsorbent, but also absolute aromaticity may be diminished, resulting in losing its adsorption capacity.

3.2. Influence of physicochemical properties of the adsorbates on adsorption: ionization and pK_a

The three EDCs and four PhACs are amphoteric species and consist of single or multiple charged groups, as well as polar groups (hydroxyl, carbonyl, carboxyl, amine, sulfonyl) with aromatic rings (benzene, isoxazole, 1,3,5-triazine, azepine). Under acidic conditions (pH 3.5), all of these EDCs/PhACs are predominantly neutral species. Increasing the pH varied the content of their ionic forms depending on each pK_a value while basic compounds lose their proton, especially for SMX, DCF, and IBP whose pK_a is relatively lower than those of other compounds. At pH values below their pK_a, the adsorption affinity toward adsorbents increased significantly with the pH, whereas the adsorption affinity dropped sharply at the pH above the pK_a values [24]. This difference occurs because the electronic coupling influences the adsorptive interaction with each adsorbent. The strong electron-withdrawing sulfonamide, carboxyl group, and hydroxyl groups on SMX, DCF/IBP, and BPA, respectively, repulse π-electron-acceptor-rich aromatic ring(s) on adsorbents [25], resulting in inhibition of π–π electron donor–acceptor (EDA) interaction, whereas less variation of adsorption affinity due to their higher pK_a values (less variation in the ionic state from neutral to ionized form) allows CBM, ATR, and EE2 to show strong hydrophobic interactions throughout a wide range of pH values (Fig. 2). Furthermore, CBM and EE2 were non-ionizable across the pH range from 3.5 to 10.5, and hence the influence of pH was negligible to the adsorption, while ATR was slightly protonated (28%) at pH 3.5, resulting in a reduction of the percent of non-ionized form (72%), [26] and an increase in the π—H bond with adsorbent.

3.3. Distribution coefficient (D)

The octanol–water partition coefficient (K_{ow}) has been used to represent hydrophobicity. This is accurate if the compounds are non-ionizable, independent of pH. However, most EDCs and PhACs in solution coexist as ionized and neutral forms across the entire pH range. Therefore, for the seven adsorbates used in this study, the use of the distribution coefficient (D) is more reasonable and preferred because it prevents the overestimation of hydrophobicity [27]. Each pH-dependent D value of EDCs/PhACs was calculated and reported in logarithmic scale at pH 3.5, 7.0, and 10.5 (Table S1). The adsorption affinity and correlation between pK_a and hydrophobicity are depicted and ordered proportionally with the hydrophobicity of adsorbate ($\log D$) in Fig. 3. Under the condition of dominant hydrophobic interaction in the adsorption study of higher-aromatic-containing adsorbents, ionized molecules hardly attract to adsorbent through this mechanism. Therefore, a sharp drop in its hydrophobicity lowers the interaction with adsorbent when pH is greater than pK_a. The variable results of adsorption capacity were observed with DCF and IBP due to their lower pK_a values (4.15 and 4.52, respectively). The higher ranked DCF and IBP in adsorption affinity at pH 3.5 dropped sharply, ranking fifth and sixth at pH 10.5, respectively, due to their declining values of $\log D$ (from 4.21 to 1.08 and 3.92 to 0.60, respectively). In contrast, the non-ionizable CBM and partially non-ionizable ATR and EE2 in basic conditions displayed less variable adsorption capacity for adsorbents, following the order of adsorption capacity, EE2 > CBM > ATR.

3.4. Adsorption difference between N-biochar and O-biochar

Hydrophobic interactions were similarly emphasized in several adsorption studies of organic compounds in various solutions [28–30]. However, the adsorption of organic chemicals cannot be interpreted by one or two mechanisms. The above results

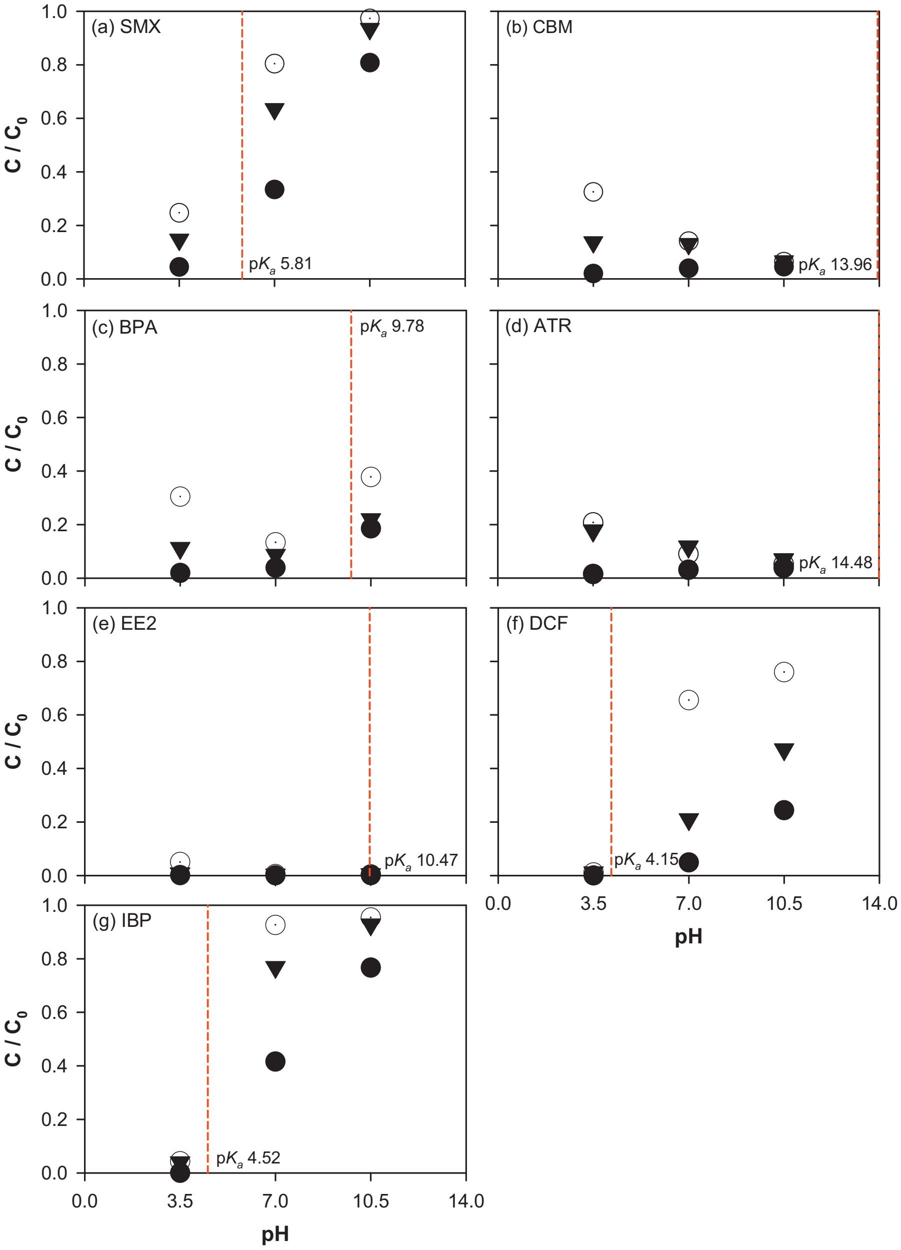

Fig. 2. Adsorption of EDCs/PhACs on each adsorbent as a function of pH, N-biochar (●); O-biochar (⊙); PAC (▼). (C_0 = 10 μM, adsorbent dose = 50 mg/L. equilibrium contact time = 7 d at 20 °C). Vertical dashed lines represent pK_a values of the respective adsorbates.

demonstrated that N-biochar allowed a higher adsorption for all seven EDCs/PhACs than O-biochar (Fig. 4), although the aromaticity of N-biochar was lower than that of O-biochar (62.5% and 74.1%, respectively). The aromaticity determined by the sum of total aromatic carbon, the aryl (108–148 ppm) and O-aryl (148–165 ppm) groups, in the ^{13}C NMR spectra increases hydrophobicity while aliphatic components cause lower aromaticity [31]. Although high aromaticity contributes to the effective adsorption, the lower surface area and pore volume of O-biochar limited the adsorption capacity than that of N-biochar (Table 1).

Elemental composition, structural characteristics, and surficial properties of biochars affect their adsorption behavior. First, the higher polarity index (O/C + N/C) and greater number of polar functional groups in the N-biochar (Table 1 and Fig. 1) indicated that the polarity of N-biochar was higher than that of O-biochar. This higher polarity of N-biochar encouraged higher adsorption affinity toward polar compounds throughout this study due to delocalization of aromatic π-cloud. This role of polarizability may lead to induced electrostatic interaction (i.e. π–π interaction, π-stacking, and London dispersion forces [32]) and the observed positive relationship between the polarities of adsorbates and the sorption coefficient, log K_{oc} (Fig. 4). The later may be interpreted by other intermolecular interactions such as dipolar and dispersion forces, resulting in higher adsorption affinity [33]. In addition, the adsorption capacity was positively correlated with the O/C fraction of both biochars, implying that the polar functional groups of N-biochar have a significant role in the adsorption of EDCs/PhACs. Moreover, larger contributions of carbohydrate (63–108 ppm), carboxyl (165–187 ppm), and carbonyl carbons (187–220 ppm) revealed by ^{13}C NMR spectra in N-biochar (Fig. 1) are attributable to the polar functional groups, indicating that a polarity provider induces the higher adsorption capacity. These polar functional groups (O-containing groups) allow H-bonding interactions for adsorbents (H-bonding donor) and chemicals (H-bonding

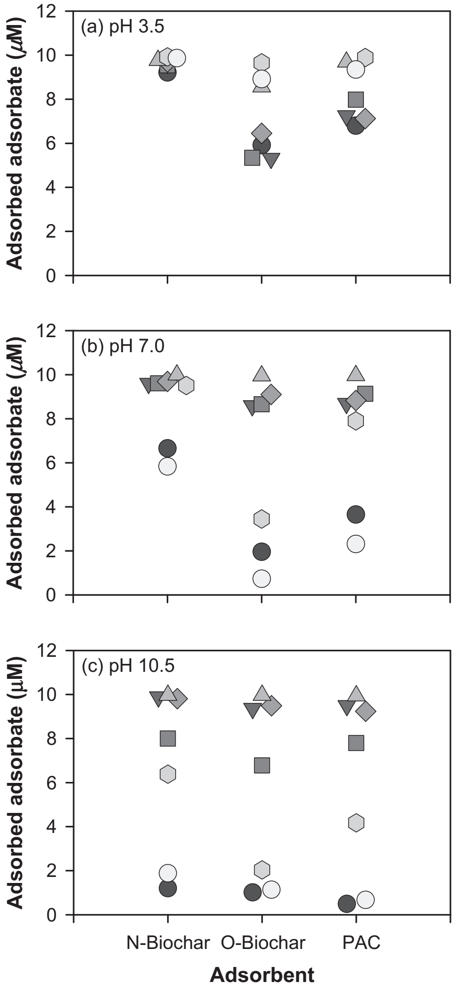

Fig. 3. Overall adsorbed EDCs and PhACs (SMX (●); CBM (▼); BPA (■); ATR (◆); EE2 (▲); DCF (⬡); IBP (○)) onto N-/O-biochars and PAC at various pH conditions; (a) pH 3.5; (b) pH 7.0; (c) pH 10.5 (C_0 = 10 μM, adsorbent dose = 50 mg/L, equilibrium contact time = 7 d at 20 °C).

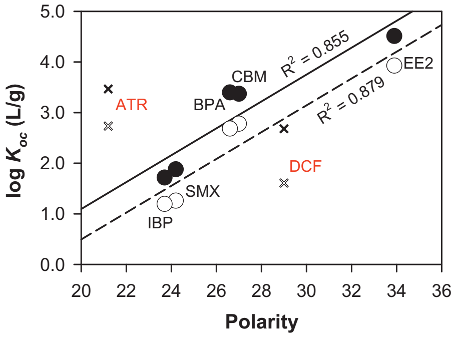

Fig. 4. Relationship between polarities of adsorbates (excluding ATR and DCF) and log K_{oc} (calculated by dividing q_e/C_e by the fraction of O/C in Table 1) at pH = 7: N-biochar (●) and O-biochar (○) (C_0 = 10 μM; adsorbent dose = 50 mg/L at 20 °C).

acceptor) [34]. The H-bonding donor groups of biochars and positively charged surface in the acidic condition (Fig. S1) enable π-H-bonding interactions with the aromatic rings of EDCs/PhACs [35]. Due to the higher portion of such O-containing functional groups on N-biochar, the adsorption activity might be attributable to π-H-bonding interactions. Moreover, this allows adsorbents possessing hydrophilic and positively charged sites to interact with ionized molecules at pH ranges between above pH of lower pK_a of adsorbates (SMX, DCF, and IBP) and each pH$_{zpc}$, although this mechanism was mostly suppressed by different values of π-electron-dependent polarizable interactions; EDA interaction, a specific non-covalent force existing between π-electron-rich moieties (π-electron donors) and π-electron-depleted moieties (π-electron acceptors) throughout the entire pH ranges [36,37]. These resulted in both a strong interaction between EDCs/PhACs (π acceptors) and the aromatic benzene-rings (π-donors) of adsorbents and hydrophobic interactions [33].

Furthermore, previous studies have proposed micropore-filling and sieving effects to elucidate the adsorption of adsorbates [25,38,39]. Different from other single-solute and bi-solute adsorptions, less pore-filling and sieving effects occurred due to the larger micro- and macro-pore volumes of N-/O-biochar (0.31 and 0.64 cm^3/g, and 0.31 and 0.32 cm^3/g, respectively). The sieving effect of all EDCs/PhACs was elucidated by result of the positive correlation between the adsorption capacity and their molecular volume; a group of ionizable compounds followed the order of adsorption capacity as DCF > IBP > SMX (Fig. S2), while that of non-ionizable compounds was determined the similar trend of order as EE2 > BPA > CBM > ATR (Fig. S3).

3.5. *Competitive adsorption among EDCs and PhACs*

The adsorption of EDCs/PhACs on biochars and PAC was regulated by the dissociable states of each adsorbate, displaying similar adsorption patterns in the order N-biochar > PAC > O-biochar. Unlike single-solute adsorption, multi-solute competitive adsorption was unable to describe the adsorption characteristics of each adsorbate through isotherm data; however, distinguishable adsorption layer type under competitive desorption was identified (Fig. S4 and Table S4). The results of overall adsorption under a gradually increasing initial concentration (10–50 μM) of each adsorbate with limited adsorption sites were able to explain the competitive adsorption (Fig. 5). The desorption was clear for ionizable compounds. For instance, DCF mostly adsorbed proportionally with increasing initial concentration of adsorbent (N-biochar, 50 mg/L) predominately under acidic condition, while dissociated DCF lost its hydrophobicity and increased its solubility, resulting in poor adsorption under neutral and basic conditions. The adsorption site allowed DCF to interact via strong hydrophobicity, impeding the multi-layer adsorption of competitive adsorbates due to its poor polarity and high π energy [14,40,41]. Unlike dissociable DCF, relatively less dissocial EE2 predominated in both the aromatic and polar functionalized sites under neutral and basic conditions via its strong hydrophobicity and higher polarity and lower π-energy, respectively [42,43]. The overall adsorbed EE2 under this condition was higher than that under acidic conditions and indicated that EE2 replaced and occupied the site at which DCF was adsorbed.

The linear Fruendlich isotherm of EE2 in Fig. S4 implies that EE2 allowed multi-layer adsorption to other competitors in terms of additional hydrogen bonding, which facilitated interactions among competitors. IBP performed similarly to the dissociable and hydrophobic pattern of DCF. Lower π-energy allowed stronger π–π EDA interactions in conjunction with hydrophobic interactions under acidic conditions; however, the former was negligible when hydrophobicity decreased sharply. ATR displayed a stable adsorption capacity toward the adsorbent under neutral and basic conditions, while it was suppressed by more hydrophobic competitors, DCF, IBP and EE2, under acidic conditions. Although the hydrophobicity of ATR was intermediate among the competitors, its lower π-energy and smaller size encouraged π-acceptors to interact with π-donors on the adsorbent, which caused a π–π EDA interaction and alleviated both the sieving effect and size-exclusion and allowed occupation of the adsorption site on the micropores

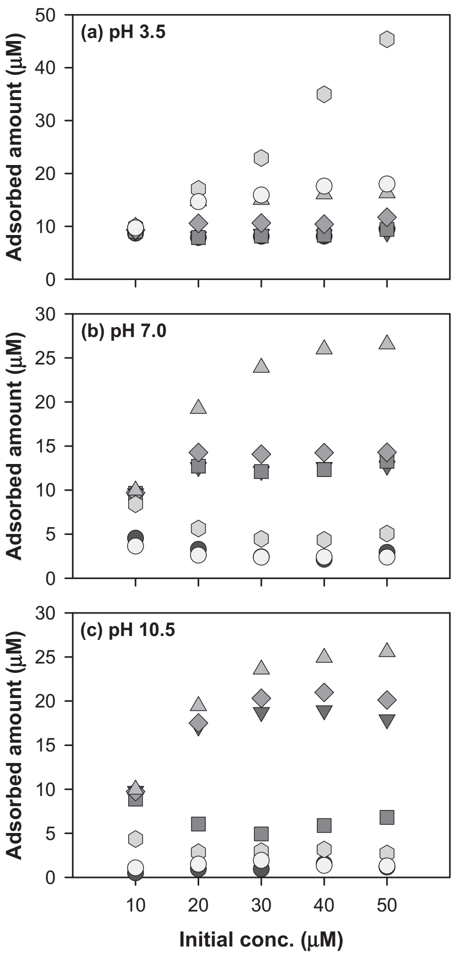

Fig. 5. Limited adsorbed adsorbates as a function of various initial concentrations (SMX (●); CBM (▼); BPA (■); ATR (◆); EE2 (▲); DCF (⬡); IBP (○)) onto 50 mg/L of N-biochar: (a) pH 3.5; (b) pH 7.0; (c) pH 10.5 (C_0 = 10–50 μM, equilibrium contact time = 7 d at 20 °C).

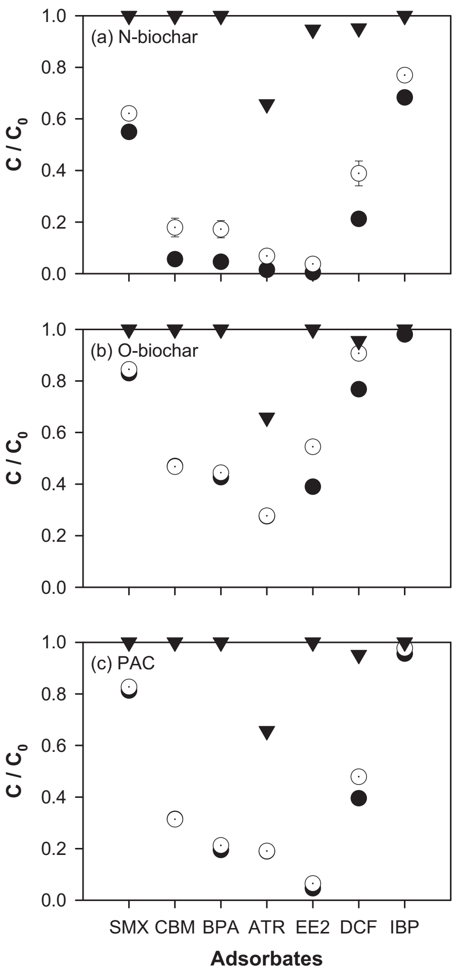

Fig. 6. Plot for NOM inhibition effect on EDCs/PhACs adsorption; in the presence (●) or absence (⊙) of humic acid, and only interaction between adsorbates and humic acid without adsorbent (▼) (C_0 = 10 μM; humic acid = 5 mg/L; adsorbent dose = 50 mg/L; pH = 7.0 at 20 °C).

[44]. The hydrophobicity of CBM was steady over a wide range of pH values due to its high pK_a 13.96, as was ATR (pK_a 14.48). This property was scarcely exhibited under conditions of coexistence with higher hydrophobic adsorbates under acidic conditions, while the relatively higher hydrophobicity resulted in strong adsorption with constant removal efficiency. The adsorption of BPA was determined to have a similar pattern to that of CBM, which was correlated with hydrophobicity, while having a slightly higher hydrophobicity than ATR and CBM with a polarity derived from two hydroxyl functional groups occupying the adsorption sites at which ATR and CBM were located under lower initial concentrations (<20 μM) (Fig. 5c). SMX exhibited inferior adsorption by virtue of its low hydrophobicity and π-energy, while the amino functional group and N-heteroaromatic rings of neutral SMX contributed to π–π EDA interactions under acidic conditions [45].

Another competitive adsorption was conducted in the presence of NOM. NOM adsorption on the adsorbent was negligible in this study. Several explanations include competition against occupying active adsorption sites and hydrophobic interaction between EDCs/PhACs and NOM. A slightly diminished adsorption capacity of chemicals was observed in the presence of NOM (Fig. 6). This explains how NOM failed not only to occupy the adsorption sites on the adsorbent, but also to interact with adsorbates in the solution, except for atrazine. NOM reduced atrazine adsorption to 34–35% under non-adsorbent conditions; this was derived from precipitation with a hydrophobic interaction between the heterocyclic aromatic ring (1,3,5-triazine) and NOM and direct site competition and pore blockage due to the small size of Atrazine [44]. Nonetheless, the predominant adsorption capacity of hydrophobic adsorbates on adsorbent was prevalent while NOM disperses not only particles [46], but also the molecules [47] in the solution or instigates ionization through interactions with diverse functional groups on NOM.

3.6. *Adsorption kinetics on adsorbents*

Adsorption kinetics are often controlled simultaneously by film diffusion and intra-particle diffusion [48]. However, the adsorption kinetics in the current study were complex due to both the mixture conditions and the desorption of compounds with weak adsorption bonding energy. Both diffusion theories barely applied to the kinetics in this study, except for the initial reaction. Thus, the tendencies of adsorption capacity and rates to reach the equilibrium concentration were investigated using the pseudo second-order model (Figs. S5 and S6, and Table S5). This well-fit pseudo second-order model implies that the rate limiting step is chemical adsorption involving electronic forces through the sharing or exchange of electrons between the adsorbent and ionized species as a function of electron donor or acceptor, respectively, regardless of equilibrium concentrations [48]. Therefore, π–π bonding and hydro-bonding interactions should be considered to evaluate the competitive adsorption in the mixture. The aromatic rings in all seven EDCs/PhACs and adsorbents form a π-system and enable π–π interactions. Due to the π-energy, calculated by the Huckel method (Table S1) [49], smaller π-energy is more reactive with higher π-energy at the atomic location [50]; the graphite form of carbonaceous adsorbents (biochars and PAC) in the order of π–π interactions was determined to be IBP > EE2 > ATR > BPA > CBM > SMX > DCF. This property correlates with adsorption capacity for hydrophobic compounds (EE2 > ATR > BPA > CBM), while that of dissociated compounds was negligible. Moreover, the steady and faster kinetic adsorption of predominantly hydrophobic compounds would occupy active pore sites so that fewer hydrophobic or ionized molecules would have the opportunity to occupy those sites.

4. Conclusion

Biochars used in this study were produced at 300 °C under controlled thermal process, which resulted in great physicochemical properties for adsorption to reduce the micro-pollutants. This controlled thermal process to produce biochar under oxygen-limited condition with simple activation allowed higher surface area and condensed aromatic carbon structure to contribute better adsorption performance. In addition, this controlled thermal process also provides efficient adsorbent, less product waste, and energy source simultaneously under tangible economical beneficial in terms of biofuel by-product use. In real aquatic environments, exposure to EDCs/PhACs occurs in either a neutral or dissociated form, resulting in specific competitive adsorption characteristics. Determination of physicochemical properties of these organic compounds; hydrophobicity, polarity, π-energy, and molecular size, and that of adsorbent; aromaticity, polarity, ash content, surface area, and the pore volume, provided better understanding of reduction of adsorbates in the aquatic system through adsorption process. Characterization of adsorbents via NMR analysis improved the interpretation of the structure and properties and allowed objective comparisons among adsorbents. Through this study, the importance of analysis both adsorbate and adsorbent is described under various attraction mechanisms and probabilities. This fundamental fate of selected micro-pollutants and an understanding of the adsorption system in biochar contribute to not only improving the removal efficiency of adsorbents, but also preventing exposure to harmful chemicals under more complex environmental conditions.

Acknowledgment

This research was supported by the Korea Ministry of Environment, ‘Project, 414-111-006’.

Appendix A. Supplementary data

Supplementary data associated with this article can be found, in the online version, at http://dx.doi.org/10.1016/j.jhazmat.2013.10.033.

References

[1] M.J. Benotti, R.A. Trenholm, B.J. Vanderford, J.C. Holady, B.D. Stanford, S.A. Snyder, Pharmaceuticals and endocrine disrupting compounds in U.S. drinking water, Environ. Sci. Technol. 43 (2008) 597–603.

[2] Y. Yoon, J. Ryu, J. Oh, B.-G. Choi, S.A. Snyder, Occurrence of endocrine disrupting compounds, pharmaceuticals, and personal care products in the Han River (Seoul, South Korea), Sci. Total Environ. 408 (2010) 636–643.

[3] D.W. Kolpin, E.T. Furlong, M.T. Meyer, E.M. Thurman, S.D. Zaugg, L.B. Barber, H.T. Buxton, Pharmaceuticals, hormones, and other organic wastewater contaminants in U.S. streams, 1999–2000: a national reconnaissance, Environ. Sci. Technol. 36 (2002) 1202–1211.

[4] J.d. Rudder, T.V.d. Wiele, W. Dhooge, F. Comhaire, W. Verstraete, Advanced water treatment with manganese oxide for the removal of 17α-ethynylestradiol (EE2), Water Res. 38 (2004) 184–192.

[5] A.M. Comerton, R.C. Andrews, D.M. Bagley, Practical overview of analytical methods for endocrine-disrupting compounds, pharmaceuticals and personal care products in water and wastewater, Philos. Trans. R. Soc. A 367 (2009) 3923–3939.

[6] L. Wackett, M. Sadowsky, B. Martinez, N. Shapir, Biodegradation of atrazine and related s-triazine compounds: from enzymes to field studies, Appl. Microbiol. Biotechnol. 58 (2002) 39–45.

[7] H. Segner, J.M. Navas, C. Schäfers, A. Wenzel, Potencies of estrogenic compounds in in vitro screening assays and in life cycle tests with zebrafish in vivo, Ecotoxicol. Environ. Saf. 54 (2003) 315–322.

[8] B. Halling-Sørensen, S. Nors Nielsen, P. Lanzky, F. Ingerslev, H. Holten Lützhøft, S. Jørgensen, Occurrence, fate and effects of pharmaceutical substances in the environment – a review, Chemosphere 36 (1998) 357–393.

[9] M. Xie, L.D. Nghiem, W.E. Price, M. Elimelech, Comparison of the removal of hydrophobic trace organic contaminants by forward osmosis and reverse osmosis, Water Res. 46 (2012) 2683–2692.

[10] T.A. Ternes, A. Joss, H. Siegrist, Scrutinizing pharmaceuticals and personal care products in wastewater treatment, Environ. Sci. Technol. 38 (2004) 392–399.

[11] C. Jung, J. Heo, J. Han, N. Her, S.-J. Lee, J. Oh, J. Ryu, Y. Yoon, Hexavalent chromium removal by various adsorbents: powdered activated carbon, chitosan, and single/multi-walled carbon nanotubes, Sep. Purif. Technol. 106 (2013) 63–71.

[12] J.E. Kilduff, T. Karanfil, Y.-P. Chin, W.J. Weber Jr., Adsorption of natural organic polyelectrolytes by activated carbon: a size-exclusion chromatography study, Environ. Sci. Technol. 30 (1996) 1336–1343.

[13] A. Ahmadpour, D. Do, The preparation of active carbons from coal by chemical and physical activation, Carbon 34 (1996) 471–479.

[14] L. Ji, Y. Shao, Z. Xu, S. Zheng, D. Zhu, Adsorption of monoaromatic compounds and pharmaceutical antibiotics on carbon nanotubes activated by KOH etching, Environ. Sci. Technol. 44 (2010) 6429–6436.

[15] W. Zheng, M. Guo, T. Chow, D.N. Bennett, N. Rajagopalan, Sorption properties of greenwaste biochar for two triazine pesticides, J. Hazard. Mater. 181 (2010) 121–126.

[16] B. Chen, D. Zhou, L. Zhu, Transitional adsorption and partition of non-polar and polar aromatic contaminants by biochars of pine needles with different pyrolytic temperatures, Environ. Sci. Technol. 42 (2008) 5137–5143.

[17] Y. Chun, G. Sheng, C.T. Chiou, B. Xing, Compositions and sorptive properties of crop residue-derived chars, Environ. Sci. Technol. 38 (2004) 4649–4655.

[18] R. Azargohar, A. Dalai, Biochar as a precursor of activated carbon, Appl. Biochem. Biotechnol. 131 (2006) 762–773.

[19] D.A. Laird, R.C. Brown, J.E. Amonette, J. Lehmann, Review of the pyrolysis platform for coproducing bio-oil and biochar, Biofuels Bioprod. Biorefining 3 (2009) 547–562.

[20] J. Park, J. Meng, K.H. Lim, O.J. Rojas, S. Park, Transformation of lignocellulosic biomass during torrefaction, J. Anal. Appl. Pyrolysis 100 (2013) 199–206.

[21] L. Joseph, Q. Zaib, I.A. Khan, N.D. Berge, Y.G. Park, N.B. Saleh, Y. Yoon, Removal of bisphenol A and 17α-ethinyl estradiol from landfill leachate using single-walled carbon nanotubes, Water Res. 45 (2011) 4056–4068.

[22] B. Hameed, A. Ahmad, N. Aziz, Isotherms, kinetics and thermodynamics of acid dye adsorption on activated palm ash, Chem. Eng. J. 133 (2007) 195–203.

[23] M. Ahmaruzzaman, Role of fly ash in the removal of organic pollutants from wastewater, Energy Fuels 23 (2009) 1494–1511.

[24] K. Yang, W. Wu, Q. Jing, L. Zhu, Aqueous adsorption of aniline, phenol, and their substitutes by multi-walled carbon nanotubes, Environ. Sci. Technol. 42 (2008) 7931–7936.

[25] L. Ji, F. Liu, Z. Xu, S. Zheng, D. Zhu, Adsorption of pharmaceutical antibiotics on template-synthesized ordered micro- and mesoporous carbons, Environ. Sci. Technol. 44 (2010) 3116–3122.

[26] ChemAxon, http://www.chemicalize.org

[27] K. Kümmerer, Pharmaceuticals in the Environment: Sources, Fate, Effects and Risks, Springer, Verlag, 2004.

[28] S. Gotovac, L. Song, H. Kanoh, K. Kaneko, Assembly structure control of single wall carbon nanotubes with liquid phase naphthalene adsorption, Colloids Surf. A 300 (2007) 117–121.

[29] K. Pyrzynska, A. Stafiej, M. Biesaga, Sorption behavior of acidic herbicides on carbon nanotubes, Microchim. Acta 159 (2007) 293–298.

[30] F. Balavoine, P. Schultz, C. Richard, V. Mallouh, T.W. Ebbesen, C. Mioskowski, Helical crystallization of proteins on carbon nanotubes: a first step towards the development of new biosensors, Angew. Chem. Int. Ed. 38 (1999) 1912–1915.

[31] K. Sun, K. Ro, M. Guo, J. Novak, H. Mashayekhi, B. Xing, Sorption of bisphenol A, 17α-ethinyl estradiol and phenanthrene on thermally and hydrothermally produced biochars, Bioresour. Technol. 102 (2011) 5757–5763.

[32] C.R. Martinez, B.L. Iverson, Rethinking the term pi-stacking, Chem. Sci. 3 (2012) 2191–2201.

[33] B. Pan, B. Xing, Adsorption mechanisms of organic chemicals on carbon nanotubes, Environ. Sci. Technol. 42 (2008) 9005–9013.

[34] K. Sun, B. Gao, Z. Zhang, G. Zhang, Y. Zhao, B. Xing, Sorption of atrazine and phenanthrene by organic matter fractions in soil and sediment, Environ. Pollut. 158 (2010) 3520–3526.

[35] D. Zhu, S. Hyun, J.J. Pignatello, L.S. Lee, Evidence for π–π electron donor-acceptor interactions between π-donor aromatic compounds and π-acceptor sites in soil organic matter through pH effects on sorption, Environ. Sci. Technol. 38 (2004) 4361–4368.

[36] C.A. Hunter, J.K.M. Sanders, The nature of pi–pi interactions, J. Am. Chem. Soc. 112 (1990) 5525–5534.

[37] C.A. Hunter, K.R. Lawson, J. Perkins, C.J. Urch, Aromatic interactions, J. Chem. Soc. Perkin Trans. 2 (2001) 651–669.

[38] D. Zhu, J.J. Pignatello, Characterization of aromatic compound sorptive interactions with black carbon (charcoal) assisted by graphite as a model, Environ. Sci. Technol. 39 (2005) 2033–2041.

[39] T.H. Nguyen, H.H. Cho, L. Dianne, W.P. Ball, Evidence for a pore-filling mechanism in the adsorption of aromatic hydrocarbons to a natural wood char, Environ. Sci. Technol. 41 (2007) 1212–1217.

[40] K. Yang, W. Wu, Q. Jing, W. Jiang, B. Xing, Competitive adsorption of naphthalene with 2,4-dichlorophenol and 4-chloroaniline on multi-walled carbon nanotubes, Environ. Sci. Technol. 44 (2010) 3021–3027.

[41] Z. Yu, S. Peldszus, P.M. Huck, Adsorption characteristics of selected pharmaceuticals and an endocrine disrupting compound—naproxen, carbamazepine and nonylphenol—on activated carbon, Water Res. 42 (2008) 2873–2882.

[42] H.-H. Cho, B.A. Smith, J.D. Wnuk, D.H. Fairbrother, W.P. Ball, Influence of surface oxides on the adsorption of naphthalene onto multi-walled carbon nanotubes, Environ. Sci. Technol. 42 (2008) 2899–2905.

[43] W. Chen, L. Duan, L. Wang, D. Zhu, Adsorption of hydroxyl- and amino-substituted aromatics to carbon nanotubes, Environ. Sci. Technol. 42 (2008) 6862–6868.

[44] Q. Li, V.L. Snoeyink, B.J. Mariãas, C. Campos, Elucidating competitive adsorption mechanisms of atrazine and NOM using model compounds, Water Res. 37 (2003) 773–784.

[45] D. Zhang, B. Pan, H. Zhang, P. Ning, B. Xing, Contribution of different sulfamethoxazole species to their overall adsorption on functionalized carbon nanotubes, Environ. Sci. Technol. 44 (2010) 3806–3811.

[46] Q. Li, B. Xie, Y.S. Hwang, Y. Xu, Kinetics of C60 fullerene dispersion in water enhanced by natural organic matter and sunlight, Environ. Sci. Technol. 43 (2009) 3574–3579.

[47] L.C. Konradt Moraes, R. Bergamasco, C.G. Tavares, D. Hennig, M. Carvalho Bongiovani, GPE 2007-utilization of the coagulation diagram in the evaluation of the natural organic matter (NOM) removal for obtaining potable water, Int. J. Chem. React. Eng. 6 (2008) A87.

[48] H. Qiu, L. Lv, B. Pan, Q. Zhang, W. Zhang, Q. Zhang, Critical review in adsorption kinetic models, J. Zhejiang Univ. Sci. A 10 (2009) 716–724.

[49] J. Cioslowski, Total π-electron energy in the variable β Hückel method, Int. J. Quantum Chem. 34 (1988) 417–421.

[50] S. Shaik, A. Shurki, D. Danovich, P.C. Hiberty, A different story of π-delocalizations: the distortivity of π-electrons and its chemical manifestations, Chem. Rev. 101 (2001) 1501–1539.